

CHAPTER 4

DISCUSSION OF RESULTS



The data of drop sizes and velocities of drop was measured by photographic experiments. Drop sizes can be estimated from equation 1 of Vedaiyan et al., equation 2 of Horvath et al., equation 5 of Skelland and Johnson, and equation 6 of Hayworth and Treybal. The drop size distribution curve compares well with the correlation of Horvath et al. and Vedaiyan et al. In this work it was found that the velocity profile of drops are paraboloidal in shape. The discussions concerning drop size, drop size distribution and velocity of drop are as follow:

4.1 Drop size

A knowledge of drop size should provide the basic information enabling the obtention of a surface area of transfer when the dispersed phase hold-up is known. Such information is needed for the design of most liquid-liquid contactors in which the drop size is related to the transfer efficiency. The most important parameters are found for predicting the drop size are nozzle velocity and nozzle diameter.

The velocities of dispersed phase through the nozzle (nozzle velocity) for distributors A, B, C and D at flow rates 3.37 cc/s were computed as 11.22, 11.92, 11.44 and 11.92 cm/s respectively. The value of the jetting velocities were calculated from equation 8 for the same distributors and for flow rates of 13.47, 10.37 7.93 and 6.01 cm/s respectively. Both computed values were compared together, showing that all nozzles form

drops by a jet breakup mechanism except distributor A, which is a single drop formation mechanism. By observing the distributor during the experiments it could be seen that drop formation is a jet breakup mechanism for all distributors and for all flow rates. One purpose of the calculation and observation is to see if it is possible to assume drop formation as a jet breakup mechanism for all distributors and for all flow rates. In such a case calculation of drop size would not be so complicated.

In drop sizes calculated by equation 6 drop diameters are smaller than the nozzle diameter and therefore equation 6 was considered not suitable. These computed drop sizes from equation 1 were compared with the experimental drop sizes, and a percentage error of about 52% was found. Scheele and Meister⁸ concluded that Hayworth and Treybal used a synthetic wetting agent to lower the interfacial tension. The effect of surfactant addition cannot be characterized solely by the resultant equilibrium interfacial tension lowering, finding maximum error of 94 and 377%. And the estimate of 10 cm/s given by Hayworth and Treybal for jetting velocity is an approximation which may be in error by more than 400%.

The calculated drop size predicted by Horvarth et al.⁵ compared well with the experimental results on distributor A and B at nozzle velocity between 23 and 29 cm/s on distributor C at all nozzle velocity, and, on distributor D the result was not satisfactory Horvarth et al. predicted the equation for calculated drop size by bridging the gap between the jetting and critical velocities, use of variables d_{jc} and v_{nc} indicated by Skelland and Johnson⁹, and concluded that the experimental to predicting d_{jc} and v_{nc} agreed with the data collected by Skelland and Johnson, and they did not say anything about the comparison of the equation for predicting

drop size with Skelland and Johnson's equation.

The drop size calculated by Vedaiyan et al.¹¹ compares well with the experimental results on distributor D however for the other distributors the agreement is not satisfactory. Vedaiyan et al. generalized the correlation by use of the functional relationship between the Sauter mean diameter and the other variables. A computer analysis was made on the experimental data to eliminate statistically insignificant dimensionless group from the correlation, this new equation compares well with their experimental results, and compared with the experimental results in this work a percentage error of about 26.80% was found.

The calculated drop size predicted by Skelland and Johnson⁹ compares well with the experimental results with a percentage error between 3.28% to 20.83%. It is believed that this equation can be used to predict drop sizes for other columns with different dispersed phase, nozzle diameter and nozzle velocity. The hydrodynamics of drops formation under jetting conditions involves many parameters such as the jet length, the jetting velocity, all of which influences the resulting drop size¹⁶. Hayworth and Treybal⁶ concluded that velocities below 30 cm/s cause increased drop size resulting from increased nozzle diameter, increased interfacial tension, decreased difference in density between the phases. Viscosity of the dispersed phases seems to have a negligible influence, and drop size was not influenced by the choice of dispersed phase.

The generalized correlation for the drop size (d_{32})

The functional relationship between Sauter mean diameter and other variables may be expressed by Vedaiyan et al.¹¹ as

$$d_{32} / \left(\frac{\gamma}{\Delta \rho g} \right)^{1/2} = c \left(\frac{v_n^2}{2gd_n} \right)^d \quad (12)$$

An analysis was made using the experimental data and giving values to c and d , the following equation is obtained

$$d_{32} / \left(\frac{\gamma}{\Delta \rho g} \right)^{1/2} = 1.552 \left(\frac{v_n^2}{2gd_n} \right)^{-0.176} \quad (13)$$

The average error in the data for the above correlation is $\pm 26.8\%$. Table 8 shows the comparison of experimental data and predicted value given by the proposed equation.

4.2 Drop size distribution

The drop size distribution was used to predicted number of actual size range, predicting the surface of transfer area when hold up is known, and study drop behavior when nozzle velocities are varied.

The pattern of distribution in all these experiments has characteristic 1, 2, 3 and 4 modes behavior. However, the monomodal occurred at low nozzle velocities and bimodal at increased nozzle velocities. Trimodal and tetramodal behavior occurred for distributor C at flow rates of 3.37 cc/s, and for distributor D at a flow rate of 8.68 cc/s respectively. Trimodal and tetramodal behavior have never been observed previously.

Vedaiyan et al.¹² and Horvath et al.⁵ concluded that size frequency based on drop number, show a change of distribution from near normal monomodal to bimodal when nozzle velocity is not greater than 30 cm/s.

Figure 45 show the relationship between d_{32} and hold-up of

Table 8 Comparison of proposed equation for predicted drop size with experimental data.

Q_d (cc/s)	Distributor A			Distributor B			Distributor C			Distributor D		
	d_{32} from Eqn. (13) mm.	d_{32} mm.	% error	d_{32} from Eqn. (13) mm.	d_{32} mm.	% error	d_{32} from Eqn. (13) mm.	d_{32} mm.	% error	d_{32} from Eqn. (13) mm.	d_{32} mm.	% error
8.68	3.60	2.55	+41.18	3.71	2.97	+24.92	3.92	3.67	+ 6.81	3.99	4.59	-13.07
6.67	3.95	2.76	+43.12	4.07	3.07	+32.57	4.30	3.77	+14.06	4.37	4.38	- 0.23
5.03	4.36	2.96	+47.30	4.49	3.38	+32.84	4.74	3.70	+28.11	4.83	4.52	+ 6.86
3.37	5.02	3.39	+48.08	5.17	3.92	+31.89	5.46	4.02	+35.82	5.56	4.56	+21.93

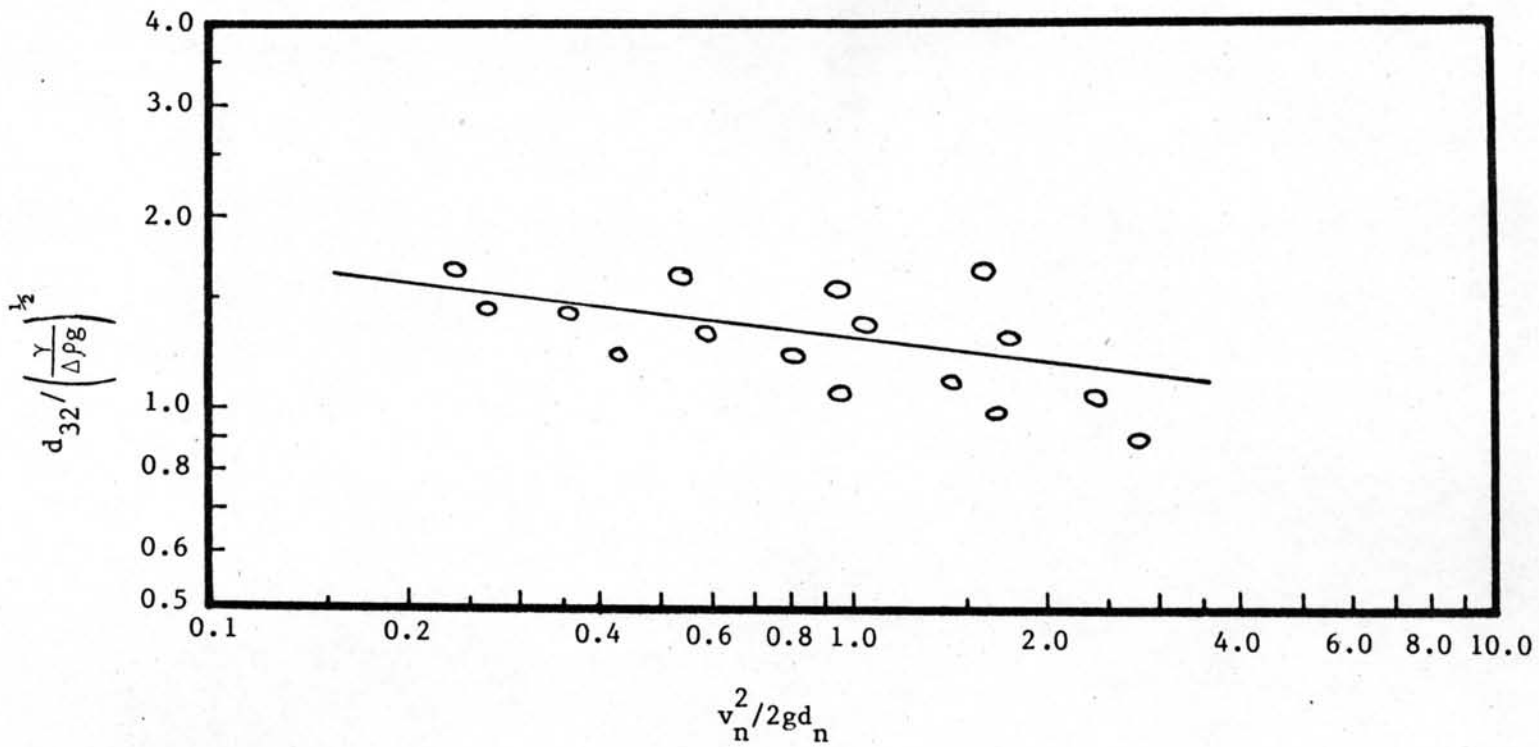


Figure 44 Generalized correlation for Sauter mean diameter

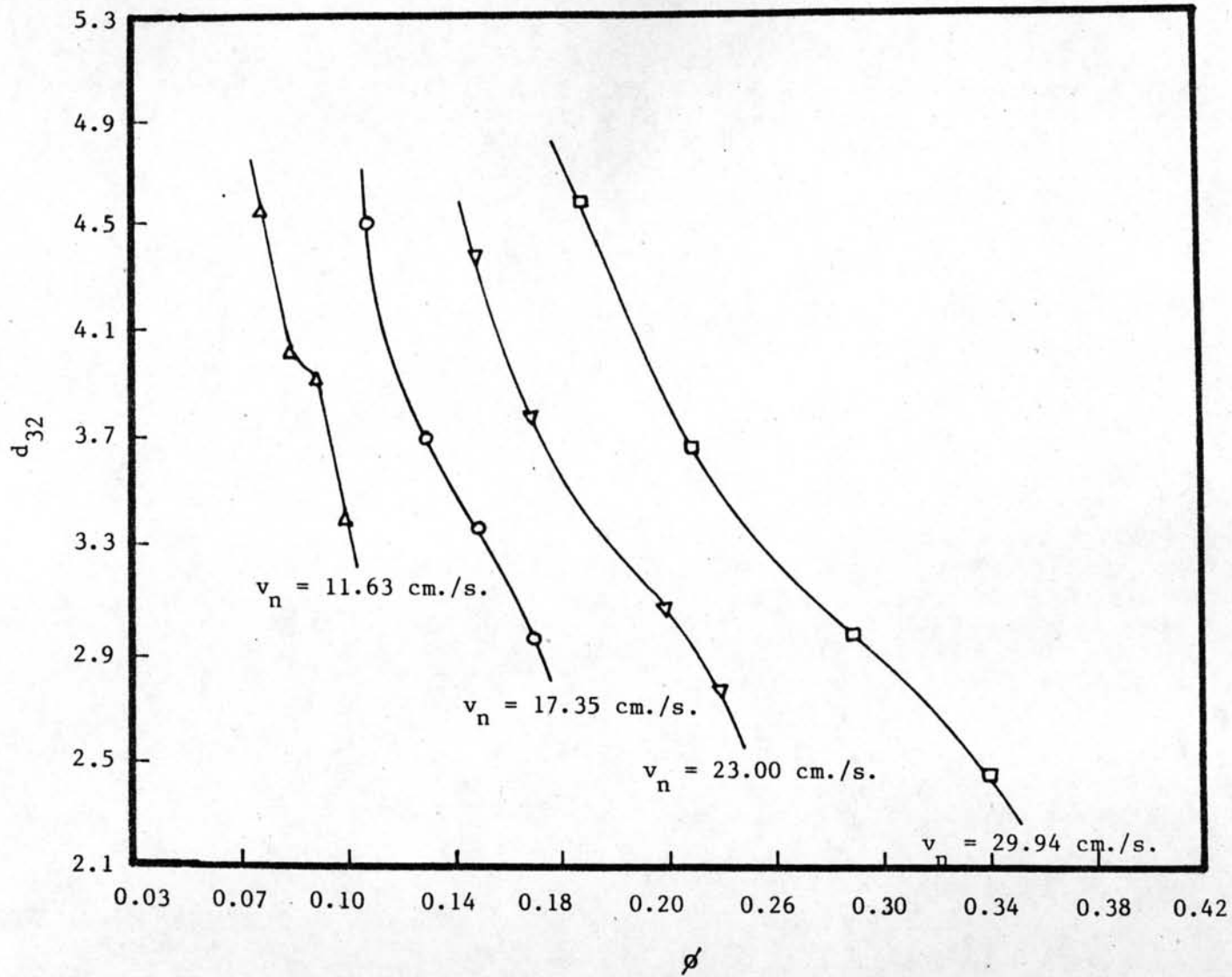


Figure 45 Computed hold-up as a function of d_{32}

dispersed phase when nozzle velocities are varied. For this reason, hold-up can be predicted when drop size and nozzle velocities are known. The hold-up is used to calculate the volume of dispersed phase in the column, thereby calculating the surface of transfer area from the size distribution curve of d_{32} .

Figure 16 shows the size distribution curve of distributor A at flow rate 3.37 cc/s, $d_{32} = 3.39$ mm., and hold-up of dispersed phase is 0.10. The calculation of surface of transfer area from d_{32} and hold-up is $2,789.96 \text{ cm}^2$., the calculation of surface of transfer area from the size distribution curve and hold-up is $2,939.72 \text{ cm}^2$., and a percentage error 5.09 is found. Figure 30 show the size distribution of distributor C at flow rates of 8.68 cc.s, the distribution curve is bimodal, $d_{32} = 3.67$ mm., and hold-up of dispersed phase is 0.23. The calculation of surface of transfer area from d_{32} and hold-up, and size distribution curve and hold-up are 5,927.33 and 6,232.80 cm^2 . respectively, the percentage error is 4.96. For these two examples the calculations to obtain the surface of transfer area using d_{32} and the hold-up and size distribution curve and hold-up were compared. The experimental values agreed. Thus, it can be concluded that the calculation of the surface area of transfer can be predicted using d_{32} or the size distribution when hold-up is known, and the surface of transfer area predicted by d_{32} has little error when predicted from the size distribution curve. The value of d_{32} calculated from the total number of drops in each run which can possibly represent the size distribution curve used to calculate the surface area of transfer.

4.3 Velocity of drop

For data No. 1 to 5 in table 7 the equation representing the average velocity profile of the drops in $y = 1.55X^{1.36}$ for d_{32} between 2.99 to 3.77 mm. and hold-up of dispersed phase between 0.17 to 0.23. For data No. 6 to 9 the general equation is $y = 0.20X^{2.54}$ for d_{32} between 3.70 to 4.60 mm. and hold-up of dispersed phase between 0.11 to 0.19. It is believed that both equations can be used to predict the velocity profiles of drop in other spray columns with the first equation being used when drop diameters are small and at high hold-ups, the second equation being used when drop diameters are large and the hold-up low.

An important piece of information in spray columns hydrodynamics is the behavior of the continuous phase. An unsuccessful attempt at measuring average continuous phase velocities as a function of radius using pitot tube measurements was made, the primary cause being a too low pressure drop on one hand and the interference of droplets entering the pitot tube on the other. As a result an indirect measurement system was tried. The velocity profile of continuous phase can be predicted by use of the relationship between terminal velocity of drops and velocity profiles of drop.

Terminal velocities can be calculated with the equations of Vigne and Hu and Kinter as shown in figures 32 to 43. For both equations, d_{43} is an important parameter to calculate terminal velocity. In figures 32 to 40 terminal velocities are shown superimposed with drop velocity profiles. In figures 41 to 43 the terminal velocities calculated by Vigne's equation are lower than the velocity profile of drop. The terminal velocities calculated by Hu and Kinter's equation are greater than the velocity profile of drop. Therefore, the average value of Vigne and Hu and

Kinter equation was used to represent the estimated terminal velocity of the drop representing the average of each run.

Experimental measurements of angles of direction of drop fall show that the average direction of drops is toward the core of the column. For this reason, it can be predicted that density of drops tend to fall down toward the core of the column. The number of drops near the axis of the column is greater than the amount of drops near the wall of the column. Therefore, the velocity profile of drops is a paraboloid with the maximum velocity being in the center.

From the average terminal velocities predicted in figure 32 to 43 it can be described that continuous phase undergoes a recirculation movement. Velocities of continuous phase around the core of the column flows downward, and near the wall of the column the continuous phase flows upward, this phenomena showed in figure 46. An expression for these flow patterns has been predicted by Wijffiels and Rietema⁴, through photographic measurement by injection of ink into the continuous phase. The velocity profile of the drops were also found to be paraboloidal in shape.

The generalized correlation for the maximum velocity of drop (v_m)

The functional relationship between the maximum velocity of drop and variables such as the nozzle diameter, d_{43} and the superficial velocity of the dispersed phase may be ascertained by dimensional analysis the approach is as follows.

$$v_m = f(v_s, d_{43}, d_n) \quad (13)$$

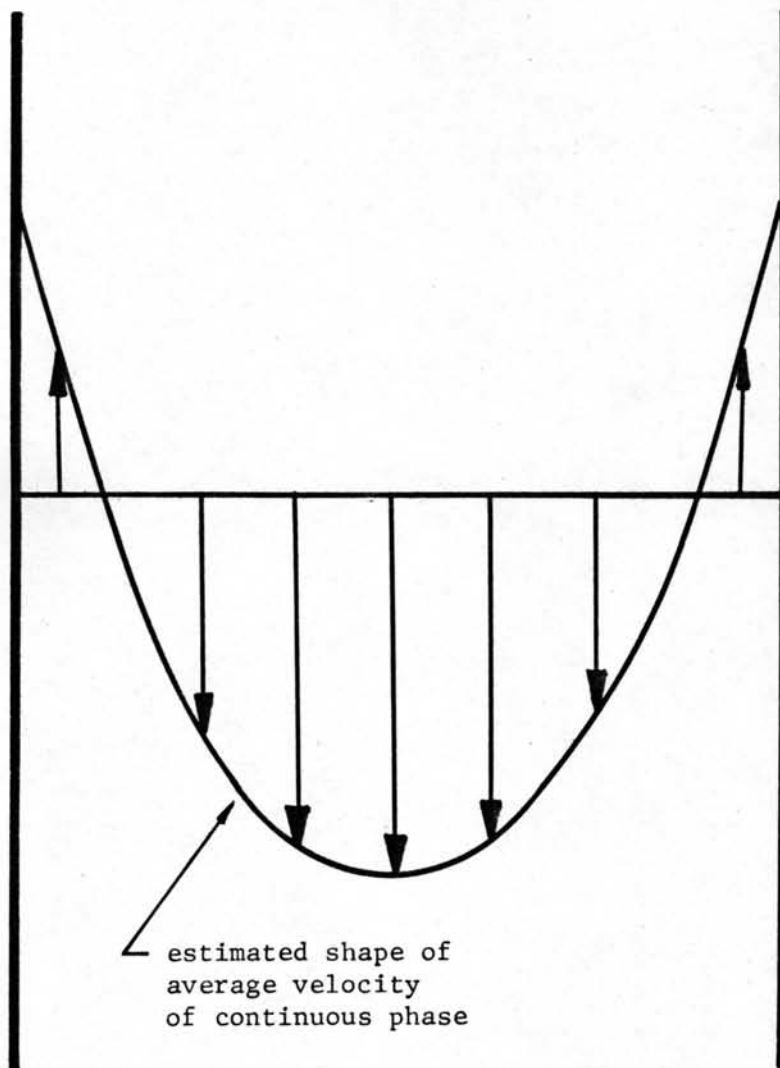


Figure 46 Continuous phase entrainment phenomena.

This equation may be transformed by dimensional analysis to the following relationship.

$$\frac{v_m}{v_s} = a \left(\frac{d_{43}}{d_n} \right)^b \quad (14)$$

An analysis was made using the experimental data to give values to a and b, resulting in the following equation.

$$\frac{v_m}{v_s} = 135.36 \left(\frac{d_{43}}{d_n} \right)^{2.67} \quad (15)$$

The average error in the data for the above correlation is $\pm 20.42\%$. Table 9 showed the comparison of experimental data and predicted value given by the proposed equation.

Table 9 Comparison of proposed equation for predicted maximum velocity of drop with experimental data.

Q_d (cc/s)	Distributor A			Distributor B			Distributor C			Distributor D		
	v_m exp. cm/s	v_m from Eqn. (15) cm/s	% error	v_m exp. cm/s	v_m from Eqn. (15) cm/s	% error	v_m exp. cm/s	v_m from Eqn. (15) cm/s	% error	v_m exp. cm/s	v_m from Eqn. (15) cm/s	% error
8.68	38.4	51.74	+34.74	40.3	34.85	-13.52	34.9	34.92	+ 0.06	33.0	38.61	-17.00
6.67	36.9	49.19	+33.31	33.9	30.43	-10.24	34.5	29.15	-15.50	30.9	26.38	-14.63
5.03	32.5	43.55	+34.00	33.0	29.37	-11.00	30.7	20.97	-31.70	30.4	21.49	-29.31



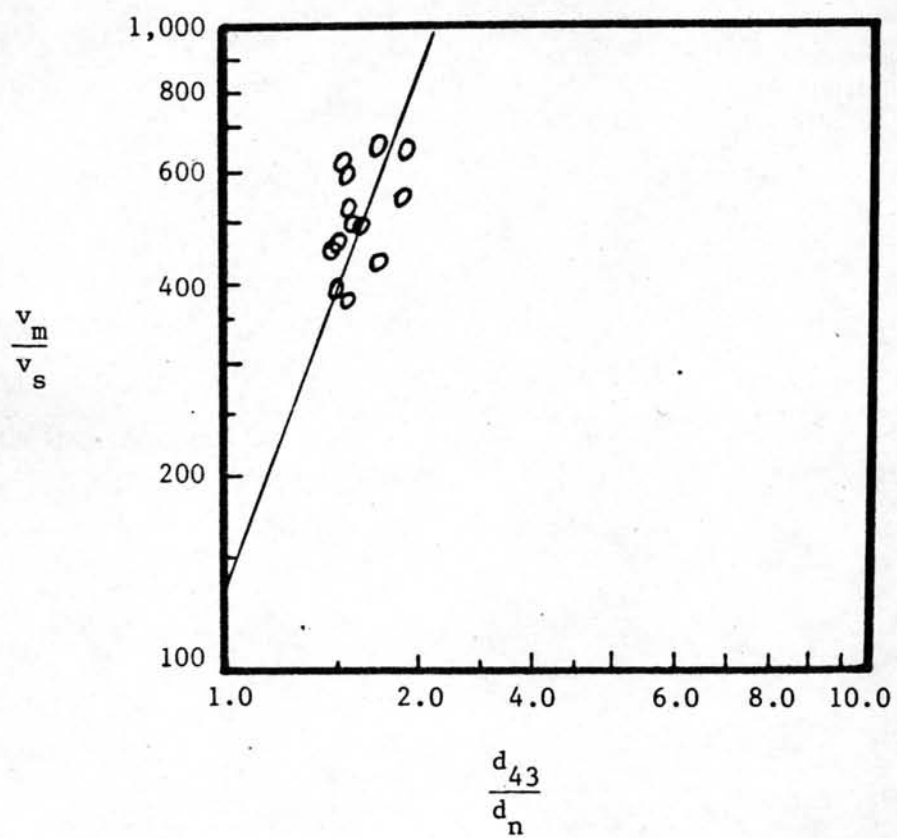


Figure 47 Generalized correlation for velocity of drop